Thermoreversible Protein Hydrogel as Cell Scaffold

Hui Yan,[†] Alberto Saiani,[†,‡] Julie E. Gough,[‡] and Aline F. Miller*[,†]

Molecular Materials Centre, School of Chemical Engineering and Analytical Science, University of Manchester, Sackville Street, Manchester, M60 1QD, United Kingdom, and School of Materials, University of Manchester, Grosvenor Street, Manchester, M1 7HS, United Kingdom

Received June 9, 2006; Revised Manuscript Received August 1, 2006

A thermoreversible fibrillar hydrogel has been formed from an aqueous lysozyme solution in the presence of dithiothreitol (DTT). Its physical properties and potential as a tissue engineering scaffold have been explored. Hydrogels were prepared by dissolving 3 mM protein in a 20 mM DTT/water mixture, heating to 85 °C and cooling at room temperature. No gel was observed for the equivalent sample without DTT. The elastic nature of the gel formed was confirmed by rheology, and the storage modulus of our gel was found to be of the same order of magnitude as for other cross-linked biopolymers. Micro differential scanning calorimetry (microDSC) experiments confirmed that the hydrogel was thermally reversible and that gelation and melting occurs through a solid−liquid-like first-order transition. Infrared spectroscopy of the hydrogel and transmission electron microscopy studies of very dilute samples revealed the presence of β-sheet-rich fibrils that were ∼4−6 nm in diameter and 1 μm in length. These fibrils are thought to self-assemble along their long axes to form larger fibers that become physically entangled to form the three-dimensional network observed in both cryo-scanning electron microscopy (cryo-SEM) and small-angle neutron scattering (SANS) studies. The hydrogel was subsequently cultured with 3T3 fibroblasts and cells spread extensively after 7 days and stretched actin filaments formed that were roughly parallel to each other, indicating the development of organized actin filaments in the form of stress fibers in cells.

Introduction

Hydrogels have recently attracted much interest in the biomaterials sector because of their ability to entrap large quantities of water or biological fluids. This high water content mimics the natural living environment, which gives them excellent biocompatibility. Moreover, their porous microstructure gives them good permeability while the three-dimensional network provides mechanical support. Consequently they have found a wide range of applications in the medical, pharmaceutical and biomaterial sectors; for example, as contact lenses,[1,2] materials for artificial organs,[3,4] and vehicles for controlled drug delivery.[5−7] Research in this area continues to grow, motivated by the need for greater understanding to allow controlled manipulation and optimization of properties.

There are three classes of molecules that can be used to produce hydrogels: polymers, peptides, and proteins. Polymers have been used extensively to create hydrogels; however, many are not adhesive to cells. Consequently recent efforts have focused on modifying the material to induce biocompatibility for tissue engineering applications by covalently or noncovalently incorporating cell-adhesion peptide sequences.[1,6−10] This process generally involves an additional synthesis step, which is polymer-specific[7,8] and can be difficult to control and distribute evenly throughout the hydrogel.[11] As an alternative, many groups are focusing on using designer peptides that form stable β-sheet-rich nanofibrils that become woven into three-dimensional hydrogels consisting of >99.5% water.[12−15] Kasai et al.[16] found that fibril structure was crucial for obtaining hydrogels with biological activity. They showed that the peptides capable of forming fibrils promoted cell attachment and neurite outgrowth, while the peptides that were unable to form fibrils did not show any biological activity. The disadvantage of using peptides is they have to be synthesized, which can be time-consuming and costly. Proteins are essentially polymers of amino acids and are known to form β-sheet-rich fibrils (nanometers in width and micrometers in length) that also further self-organize and entangle to form three-dimensional hydrogels under appropriate conditions.[17−20] It is thought that the fibrillar network is stabilized by intermolecular and/or intramolecular hydrogen bonding, electrostatic interactions, and hydrophobic effects. They are readily available and material properties can be manipulated easily by varying the amino acid sequence, changing the environmental conditions and/or incorporating small bioactive peptide sequences into the material. To date the potential of proteins as structural elements in material design has yet to be fully realized.

In this work, we have focused on the gelation behavior of the model protein hen egg white lysozyme (HEWL) in the presence of a reductant, dithiothreitol (DTT), in aqueous solution. This protein is a small globular protein and contains both α-helix and β-sheet in its secondary structure and has high solubility in water. Transparent viscoelastic gels were formed under physiological conditions at water contents as high as 97% (w/w), and their formation was found to be thermoreversible. Such gels alone exhibited good biocompatibility when they were cultured with fibroblast cells, showing for the first time that protein hydrogels could be used as scaffolds for tissue engineering.

Experimental Section

Materials. Hen egg white lysozyme (HEWL) was purchased from Sigma and used without further purification. The desired quantity of

* Corresponding author: telephone +44 161 3065781; fax +44 161 3064399; e-mail Aline.Miller@manchester.ac.uk.

[†] Molecular Materials Centre, School of Chemical Engineering and Analytical Science.

[‡] School of Materials.

10.1021/bm0605560 CCC: $33.50
Published on Web 09/21/2006

protein (3 mM; 42.9 mg mL^{-1}) was dissolved in doubly distilled water with 20 mM reductant dithiothreitol (DTT) (Fluka) and agitated for 60 s by use of a vortex mixer. This solution was either used immediately for characterization experiments or incubated for 10 min at 85 °C and subsequently cooled at room temperature. Resulting gels were then refrigerated at 5 °C until required for cell culture experiments for periods up to 1 week.

Micro Differential Scanning Calorimetry. MicroDSC measurements were performed on a Setaram micro differential scanning calorimeter III. The instrument was calibrated by use of the Setaram "Joule effect" calibration module supplied with the instrument. Setaram standard stainless steel matching cells with known weight were used. The sample cell was filled initially by introducing 0.5−0.6 mL of solution by use of a micropipet. The cell was then sealed hermetically. The reference cell was subsequently filled and its weight was adjusted by use of a micro balance to ensure an identical mass of solution was present in both the sample and reference cells. The solutions in which lysozyme were dissolved, that is, pure water or DTT/water mixture, were used as the references. Both cells were weighed before and after each experiment to ensure no loss of material occurred through evaporation. The microDSC thermographs were recorded with a 1.0 °C min^{-1} scanning rate in the temperature range 10−90 °C. A minimum of three heating and cooling cycles were performed for each sample, and each measurement was repeated at least 3 times to ensure reproducibility. Analysis of the thermographs was carried out by use of the Setaram Soft 2000 software supplied with the instrument. For comparative purposes all microDSC data have been normalized by the sample weight and plotted on the same scale.

Mechanical Properties. Rheological studies were undertaken by use of a stress-controlled rheometer (Bohlin C-CVO). Parallel plates (20 mm diameter) with a 0.5 mm gap were employed for all samples. Sample (1 mL) was loaded onto the stage and the upper plate was slowly lowered until the desired gap between plates was reached. The excess solution was then soaked away. To minimize solvent evaporation at elevated temperatures, a thin layer of paraffin oil was placed around the periphery of the exposed sample and a solvent trap was used with wet tissue placed inside. To ensure the rheological measurements were done in the linear regime, a strain sweep at 2π rad s^{-1} was performed. It showed no variation in G' and G'' up to a strain of 10%. Two types of rheological experiments were performed: frequency sweeps were carried out on gels between 10^{-2} and 10^{2} rad s^{-1} at 25 °C, and temperature scans were performed by setting frequency and strain at 2π rad s^{-1} and 1%, respectively. The changes in the elastic and viscous moduli were measured between 25 and 85 °C at 1 °C min^{-1}. All measurements were repeated at least three times to ensure reproducibility.

Fourier Transform Infrared Spectroscopy. Fourier transform infrared spectra were collected in transmission mode on a Nicolet Avitar 360 FTIR spectrometer. Aliquots of incubated gel samples prepared in D_2O were placed between CaF_2 windows with a 50 μm thick Teflon spacer. Cell temperature was maintained at 25 °C by connecting to a Fisher BC 10 water bath. For each sample 32 scans were collected and averaged in order to obtain a good signal-to-noise ratio. Spectra of pure D_2O and the D_2O/DTT mixture were also collected as background and subtracted from the sample spectra.

Transmission Electron Microscopy. Transmission electron microscopy (TEM) experiments were performed on a CM200 TEM from Philips at 200 kV accelerating voltage. To investigate the fibrillar structure of our material, gels were diluted 20-fold and agitated vigorously to separate the fibrils. A 5 μL drop of the resulting solution was applied to a carbon-coated Formvar grid, blotted after 60 s, and left to air-dry. A 5 μL drop of 2% (w/v) uranyl acetate (Agar Scientific) solution was subsequently placed on the grid, blotted after 30 s, air-dried, and examined under the TEM.

Cryo-Scanning Electron Microscopy. A drop of gel was placed between two miniature rivets on a vacuum transfer rod and the sample was slam-frozen in a nitrogen slush and transferred to the cryostat chamber, which was maintained at − 150 °C. The top rivet was flicked off to produce a fractured surface, the ice was sublimed at − 90 °C, and the fractured surface was coated with gold/palladium. The sample was then transferred to the microscope chamber, which was also maintained at − 150 °C. Sample microstructure was probed by use of a FEI XL30 ESEM FEG at 20 kV accelerating voltage operating at high vacuum.

Small-Angle Neutron Scattering. Small-angle neutron scattering (SANS) experiments were carried out at Forshungszentrum Jülich, Germany, on beamline KWS2. A wavelength of $\lambda = 0.48$ nm was used with a wavelength distribution characterized by a full width at half-maximum $\Delta\lambda/\lambda = 10\%$. The beamline is equipped with a two-dimensional detector with a 50 × 50 cm^2 active area with a spatial resolution of 0.8 × 0.8 cm^2 (further details are available on request at Forshungszentrum Jülich). By varying the sample−detector distance, the available momentum transfer vector (q) was in the range of $0.1 < q$ (nm^{-1}) < 2.0, with $q = (4\pi/\lambda) \sin(\theta/2)$, where θ is the scattering angle. Counter normalization was achieved by using the incoherent scattering of an amorphous hydrogenous poly(methyl methacrylate) standard provided. The normalized intensity was then subtracted for the empty cell and the solvent scattering. Gel samples for neutron scattering were prepared as described above directly in a Hellma quartz cell of 2 mm thickness. Deuterated water (D_2O) was used instead of hydrogenated water in order to increase the contrast between the protein and the solvent.

Cell Culture. Mouse NIH 3T3 fibroblasts (ECACC 95082219) were cultured in Dulbecco's modified Eagle's medium (DMEM) containing 10% fetal bovine serum (FBS) and 1% penicillin/streptomycin. Cells were maintained in a humidified incubator at 37 °C with 5% CO_2. All cell culture reagents were obtained from Invitrogen, U.K. Gels were loaded into a 24-well tissue culture plate (0.5 mL gel $well^{-1}$) and subsequently sterilized by irradiation with UV light for 30 min before seeding with 40 000 cells mL^{-1} on the gel surface. Cell morphology was followed with a Leica light microscope.

Environmental Scanning Electron Microscopy. Samples were examined after cell culture by removing the cell culture media, extracting the gels from the culture place, and placing a drop on a copper stub inside the microscope chamber of an FEI Quanta 200 ESEM. The samples were left to equilibrate at 5 °C (temperature controlled by a Peltier device under the copper stub). A few drops of distilled and deionized water were placed around the sample, before the chamber was sealed and evacuated to an initial pressure of 8 Torr. The chamber was flooded several times with water vapor before the chamber pressure was reduced to ∼6 Torr. Images were subsequently taken at an accelerating voltage of 10 kV.

WST-1 Assay for Cell Proliferation. Cells were cultured for 1, 4, and 7 days. Prior to each measurement, the cell culture medium was removed and samples were rinsed twice with phosphate-buffered saline (PBS) before addition of fresh cell culture medium. WST-1 reagent (59.4 μL; Roche Applied Science) was subsequently added into each well. After incubation for 4 h, the absorbance of the samples was recorded by use of a LabSystems Ascent colorimetric plate reader at 450 nm, with a reference wavelength of 620 nm. The background of the WST-1/cell culture medium mixture was subtracted and the actual cell number calculated by comparing values obtained with the standard WST-1-cell number curve.

Fluorescence Microscopy. Culture medium was removed and samples were rinsed with PBS. Paraformaldehyde (4%) was used to fix cells before 0.1% Triton 100 was used to permeabilize the cells. After the cells were washed with PBS/1% BSA, actin filaments were stained with 20 μg mL^{-1} FITC-phalloidin (Sigma, U.K.) in PBS for 20 min at room temperature and then rinsed with PBS. Samples were mounted under glass coverslips with a drop of Prolong Gold antifade reagent containing DAPI (Invitrogen, U.K.). Samples were subsequently mounted on the sample holder and examined with a Nikon fluorescence microscope.

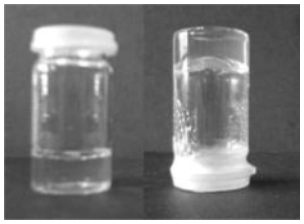

Figure 1. Lysozyme solution (3 mM) in the presence of 20 mM reductant (left panel) before and (right panel) after a heating/cooling cycle.

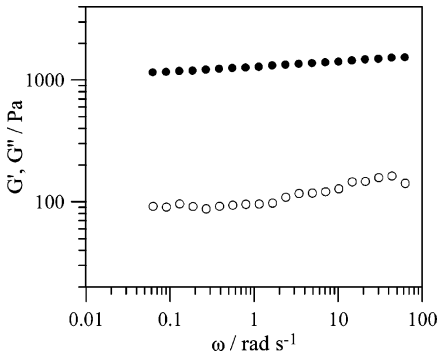

Figure 2. Mechanical spectrum of a 3 mM cured lysozyme gel at 25 °C with small oscillatory shear in the linear viscoelastic regime: (●) G'; (○) G''.

Results and Discussion

To investigate the effect of DTT on the behavior of lysozyme, we prepared two 3 mM lysozyme solutions: one in pure water and the second in a 20 mM DTT/water mixture. Both solutions had a pH of 6.9 and were heated to 85 °C, incubated for 10 min, and then cooled slowly to room temperature. A clear gel, which did not flow upon inversion of the vial (see Figure 1), was obtained in the presence of DTT, while the solution with only protein did not change. This solution was subsequently incubated at 85 °C for a further 14 days, cooled again to room temperature, and left overnight. Still no gel was obtained. This simple experiment highlights the key role played by the reductant in the formation of lysozyme hydrogels under mild conditions.

Figure 2 shows a mechanical spectrum performed at room temperature for the gel prepared in the presence of DTT. The storage modulus (G') is found to be approximately an order of magnitude larger than the loss modulus (G''), indicative of an elastic rather than viscous material. Both G' and G'' are essentially independent of frequency over the range $10^{-2}-10^{2}$ rad s^{-1}, which indicates the dominant viscoelastic relaxations of the network are at lower frequencies; that is, the relaxation time, τ, of the network is long. Such rheological behavior matches the characteristic signature of a solidlike gel. The value obtained for G' (~1000 Pa) is of the same order of magnitude as the modulus reported in the literature for other cross-linked biopolymer hydrogels including actin and agarose.[21] It should be emphasized, however, that our gels are not chemically cross-linked. They are thermoreversible and can be melted and re-formed simply by heating and cooling the sample, which is a characteristic exhibited by networks thatare physically cross-linked through weak cooperative interactions that can be disrupted at high temperature, for example, hydrogen-bonding, electrostatic, or hydrophobic interactions.[27]

Thermal Behavior. The thermal behavior of the lysozyme solutions prepared in both pure water and DTT/water mixture was investigated by microDSC. Typical thermographs for the first two heating/cooling cycles are shown in Figure 3.

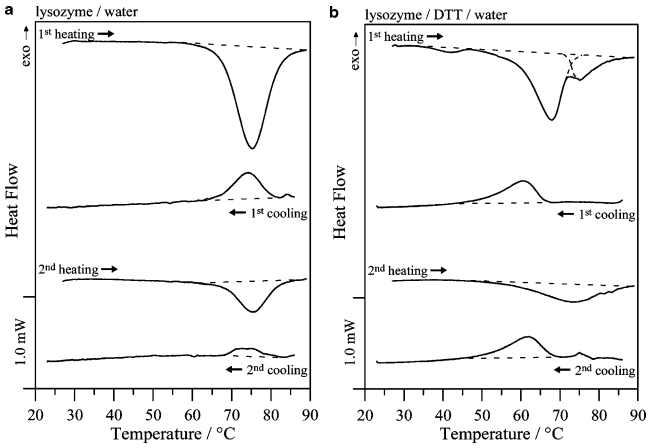

Figure 3. Micro DSC curves of a 3 mM lysozyme sample in (a) pure water and (b) a DTT/water mixture during two heating/cooling cycles. Heating and cooling rate was 1.0 °C min^{-1}.

For the protein sample in pure water a single endothermic peak is observed at 75.8 ± 0.5 °C (Figure 3a and Table 1) during the first heating run, which has previously been associated with the denaturation of native lysozyme.[22] On cooling, an exothermic transition is observed at the same temperature (Figure 3a). The enthalpy of this exotherm, 290 ± 10 mJ g^{-1}, is smaller than the denaturation enthalpy observed during the first heating, 1280 ± 30 mJ g^{-1}. As said previously, no gel formation is observed in this system, hence this exotherm is thought to be due to the partial renaturation of lysozyme. During the second heating the denaturation transition of lysozyme is again observed at the same temperature (Figure 3a). As expected, the denaturation enthalpy in this case, 440 ± 20 mJ g^{-1}, is lower that the one measured during the first heating and is similar to the renaturation enthalpy observed during the first cooling. The differences in denaturation and renaturation enthalpies during the first heating and the first cooling and second heating suggest, if it is assumed that 100% of the protein has denatured during the first heating, only 23~34% of lysozyme renatures during the first cooling, while the rest has denatured irreversibly. On the second cooling, partial renaturation of the protein is again observed and the renaturation enthalpy is reduced further, 90 ± 10 mJ g^{-1}. This behavior suggests that, during each heating, a portion of the lysozyme is denatured irreversibly, and as the number of heating/cooling cycles increases, more lysozyme denatures irreversibly. During the third cooling almost no renaturation is observed as shown by the enthalpy reported in Table 1 (where all the microDSC data are summarized), suggesting that almost all the protein has denatured irreversibly.

For the solution prepared in DTT/water mixture, three endothermic transitions are observed during the first heating at 41.7 ± 0.5, 67.8 ± 0.5, and 74.5 ± 0.5 °C (Figure 3b and Table 2). Lysozyme contains four disulfide bonds that are known to be disrupted by the presence of DTT reductant.[23] This results in the protein backbone becoming more flexible, allowing partial unfolding of the native protein. The first endothermic transition detected at 41.7 ± 0.5 °C is thought to be due to this partial unfolding of lysozyme. The increase in backbone flexibility also results in lowering its stability, and both the temperature and energy required to denature the protein decrease in comparison to a pure lysozyme solution. Indeed the denaturation peak at 67.8 ± 0.5 °C is reproducibly ~8 °C lower and has a lower associated enthalpy, 830 ± 40 mJ g^{-1}, in comparison to the lysozyme solution prepared without reductant, 1280 ± 30 mJ g^{-1}. Such phenomena have been observed previously for HEWL in concentrated ethanol solutions[24,25] and for variants of wild-

Table 1. Micro Differential Scanning Calorimetry Results for 3 mM Lysozyme Protein Solution in Pure Water

	heating			cooling		
	run 1	run 2	run 3	run 1	run 2	run 3
onset temperature, °C	67.7 ± 0.5	68.7 ± 0.5	65.8 ± 0.5	79.5 ± 0.5	68.2 ± 0.5	68.6 ± 0.5
peak temperature, °C	75.8 ± 0.5	75.3 ± 0.5	74.3 ± 0.5	74.3 ± 0.5	61.1 ± 1.0	62.6 ± 1.6
enthalpy, mJ g^{-1}	1280 ± 30	440 ± 20	110 ± 10	290 ± 10	90 ± 10	40 ± 10

Table 2. Micro Differential Scanning Calorimetry Results for 3 mM Lysozyme Protein Solution in a 20 mM DTT/Water Mixture

	heating					cooling		
	run 1, 1st transition	run 1, 2nd transition	run 1, 3rd transition	run 2	run 3	run 1	run 2	run 3
onset temperature, °C	37.6 ± 0.5	59.2 ± 0.5	69.2 ± 0.5	60.2 ± 0.5	62.8 ± 0.5	66.1 ± 0.5	68.2 ± 0.5	68.6 ± 0.5
peak temperature, °C	41.7 ± 0.5	67.8 ± 0.5	74.5 ± 0.5	73.4 ± 0.5	74.5 ± 0.5	60.3 ± 0.5	61.1 ± 1.0	61.7 ± 1.6
enthalpy, mJ g^{-1}	32 ± 1	830 ± 40	250 ± 10	440 ± 10	440 ± 10	300 ± 20	300 ± 20	300 ± 20

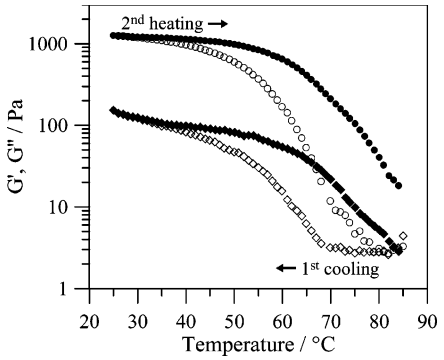

Figure 4. Viscoelastic behavior of a 3 mM lysozyme DTT/water sample during initial cooling (from 85 to 20 °C) and second heating (from 20 °C to 85 °C) at 1 °C min^{-1}: (○) G' and (◇) G'' upon cooling; (●) G' and (◆) G'' upon heating.

type human lysozyme, where substituting specific key amino acids disrupted the hydrogen-bonding network in the native form.[26] The temperature of the additional endothermic transition observed at 74.5 ± 0.5 °C coincides with the denaturation transition for lysozyme without DTT. The exact origin of this transition is not clear to us at this point. It is known that DTT does not fully disrupt all disulfide bonds of the protein in ethanol solutions, hence this peak could originate from the denaturation of residual native protein or from unfolding of the inner, nondenatured structure if the hydrophilic DTT did not disrupt the disulfide bonds present in the hydrophobic interior of the protein.[22] It should be noted that the enthalpy of this transition is small, indicating that the majority of protein has been affected by DTT. Alternatively, it could be due to the melting of aggregates or links formed during the first heating of the sample. As we will see, its temperature is in the melting range of the lysozyme gels.

During the subsequent cooling of the lysozyme solution prepared in the presence of DTT, a single exothermic transition at 60.3 ± 0.5 °C is observed (Figure 3a). This transition temperature is 14 °C lower than the one observed in the lysozyme/water system (Figure 3b) and correlates well with the macroscopic gelation temperature observed by visual inspection of the sample on cooling. This suggests that the transition corresponds to the gelation of the lysozyme/DTT/water system. This is also confirmed by our rheological measurements. In Figure 4 the storage and loss moduli of the sample are shown as a function of temperature during the first cooling of the lysozyme/DTT/water system. As can be seen, a large increase in the storage and loss moduli is observed from 68 to 45 °C. This temperature range is in very good agreement with the temperature range in which the gelation exotherm is observed by microDSC (see Figure 3b). No renaturation peak is observed in microDSC during the first cooling and no further denaturation transition occurs during the second heating of the sample, suggesting that in the presence of DTT the denaturation of lysozyme is complete after the first heating. This is probably due to the partial unfolding of the protein resulting from the disulfide bonds disruption caused by DTT, making the native protein less stable and more prone to denaturation. These results validate that denaturation of lysozyme is irreversible under these conditions.

On the second heating in microDSC, a single broad endothermic transition that stretches over 35 °C is observed at 73.4 ± 0.5 °C. This corresponds to the macroscopic melting of the gel, and the transition temperature is in good agreement with the macroscopic melting temperature observed by visual inspection of the sample during heating. This type of broad melting endotherm is often observed for hydrogels.[27] Once again this is confirmed by the rheological data. As shown in Figure 4, there is a significant decrease in G' and G'' from 55 °C onward during the second heating of the sample. At 85 °C G' is still decreasing and has not reached the value recorded before the first cooling. This is due to the gel not being fully melted at 85 °C, while during the first cooling the system does not begin to gel until 70 °C; consequently it is still a liquid at 85 °C. This is confirmed by the microDSC thermograph, where it is clear that the melting transition of the gel is not complete until 90 °C (see Figure 3b). It should be noted that there is again good agreement between the rheological and thermal measurements as the melting temperature range observed is the same for both methods. Both methods also show the presence of a 10−20 °C hysteresis between the gelation and the melting of the sample. This type of hysteresis is often observed for hydrogels.[27]

On further cooling and heating, the same gelation and melting transitions were observed. The temperatures and enthalpies obtained are reproducible as shown in Tables 1 and 2. These results suggest that our system is indeed thermoreversible and the gel can be melted and re-formed by simple heating and cooling of the sample. Our results also show that gelation and melting occurs through first-order transitions indicative of a solid−liquid-like transition.

Structure and Morphology. It has been shown that lysozyme can form fibrils that are rich in β-sheet structure upon denaturation under conditions where the protein unfolds through a partially structured intermediate.[24−26] Recent simulation studies support this view.[28] To investigate the presence of β-sheet fibrils in our systems, the samples obtained after incubation for 10

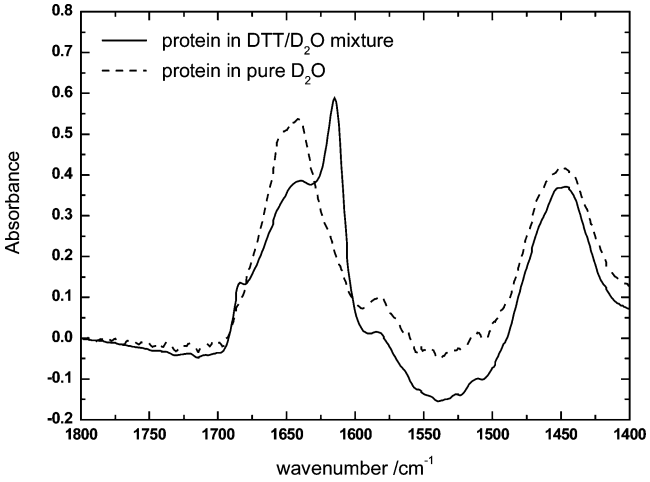

Figure 5. Fourier transform infrared spectra for 3 mM incubated protein prepared in pure D_2O (– – –) and a DTT/D_2O mixture (—).

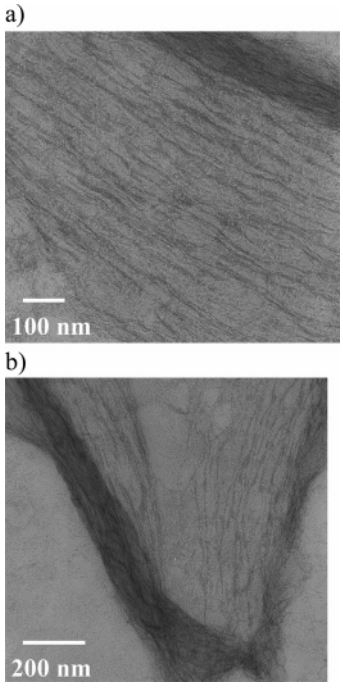

Figure 6. Transmission electron micrograph of negatively stained fibrils from a 20-fold diluted 3 mM lysozyme hydrogel in the presence of DTT where the scale bar represents (a) 100 nm and (b) 200 nm.

min at 85 °C were examined by Fourier transform infrared spectroscopy (FTIR) and transmission electron microscopy (TEM). The FTIR spectrum of the protein/DTT/water mixture (Figure 5) shows two additional peaks, in comparison to the protein/water system, at 1616 and 1684 cm^{-1}, which are indicative of intermolecular antiparallel β-sheet structure.[29] These results show that β-sheet fibrils are formed in the presence of DTT only. To observe the fibrils under TEM, a gel prepared in DTT/water mixture was diluted 20-fold in water and agitated vigorously to separate the fibrils. A typical TEM micrograph is given in Figure 6a. As can be seen, very thin fibrils of ~4−6 nm diameter and ~1 μm in length are observed. No such fibril could be observed for the sample prepared in pure water. This suggests that the disruption of the disulfide bonds, which is known to stabilize the partially folded state, is a prerequisite to the fibrillation of lysozyme. When pure water is used, the disulfide bonds are not disrupted and consequently this does not allow fibril formation; hence a portion of the protein simply renatures upon cooling. The fibrils in TEM appear short and

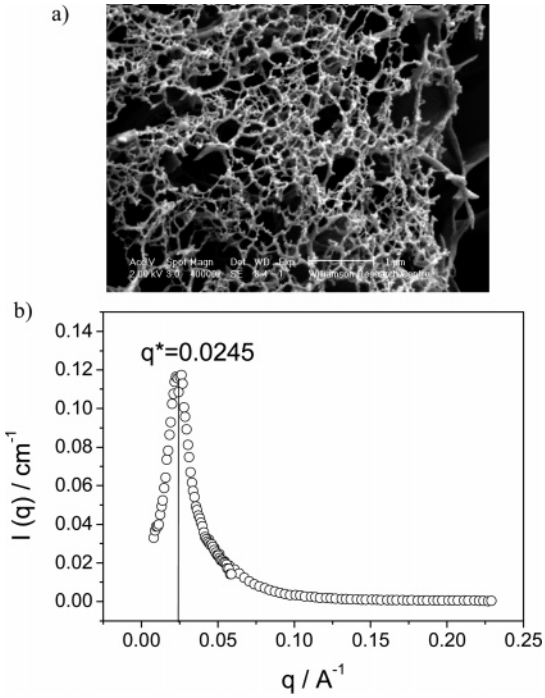

Figure 7. Microstructure of a 3 mM lysozyme DTT/water hydrogel: (a) cryo SEM micrograph of the gel network and (b) SANS scattering curve at 25 °C.

stiff and would not be expected to entangle and form a 3D network. However, it is likely as suggested by Figure 6b that these fibrils align along their long axes and cluster to form larger fibrillar structures.

The morphology of the hydrogel was examined by cryo-scanning electron microscopy (cryo-SEM), and a typical micrograph is shown in Figure 7a. It is evident that long fibers have formed and become entangled to form a three-dimensional network. The length and width of the fibers observed here seems to be bigger than the single fibrils observed by TEM (Figure 6), reinforcing the earlier postulation that individual fibrils self-assembled to form larger fibers that can form the physical cross-links that create the three-dimensional network. Fiber width was estimated to be ca. 10−20 nm. It is difficult to extract accurate dimensions from such cryomicrographs due to the introduction of artifacts and sample movement during preparation; consequently we turned to small-angle neutron scattering (SANS), where contrast was obtained by dissolving protein in a DTT/D_2O mixture. To ensure that D_2O does not adversely affect our system, microDSC experiments were performed on gels prepared in a D_2O/DTT mixture. The same transitions, shifted by 4 °C to higher temperatures, were observed, indicating that the system is not affected or only weakly affected by the substitution of protonated by deuterated water. The scattering curve obtained at 25 °C is given in Figure 7b. A scattering maximum was observed at a q^* value of 0.245 nm^{-1}. Neutron scattering is sensitive to the difference in scattering density between phases, in our case the scattering density difference between the protein-rich phase, the network, and the protein-poor phase, the solvent. Scattering patterns for multiphase systems are a complex function of the structure and the arrangement of the different scattering phases. A rigorous interpretation of the origin of a single scattering peak in a SANS curve can be made only for specific arrangements and structures. In our case only an estimated value of the average size of the scattering density fluctuation of the observed morphology, d, can be obtained from the position of the peak maximum, q^*, through the Bragg

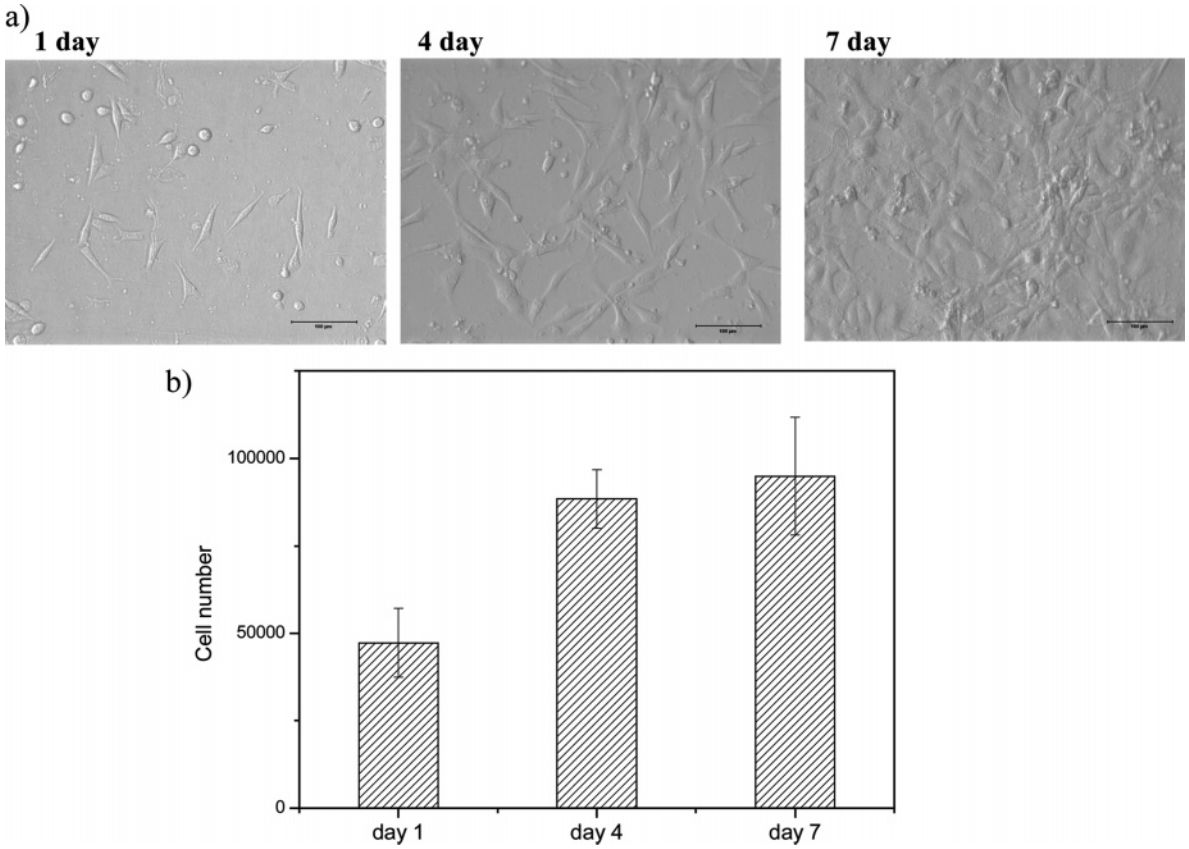

Figure 8. Cell attachment and spreading after seeding (40 000 cells well^{-1}) on 3 mM lysozyme DTT/water gels: (a) inversion light microscope images where the scale bar represents 100 μm, and (b) quantified cell number at 1, 4, and 7 days (for days 1−4, $p < 0.0025$; for days 4−7, $p < 0.05$).

relation:[30]

$$d = \frac{2\pi}{q^*} \tag{1}$$

d can be seen as an estimate of the network mesh size and is 25.6 nm for our system. The narrow shape of the scattering maximum observed also suggests the presence of a regular network with a relatively uniform mesh size.

Our structural work suggests that lysozyme in a DTT/water mixture denatures irreversibly through a partially folded state to form very thin β-sheet-rich fibrils. These fibrils seem to aggregate in larger fibers that physically cross-link through lateral interactions and form the three-dimensional network of the hydrogel. The melting and gelling transitions observed by microDSC are believed to be due to the disruption and formation of the three-dimensional network formed by these larger fibers.

Cell Attachment, Spreading, and Proliferation. To investigate cell−hydrogel interactions, cured lysozyme gels were cultured with 3T3 fibroblasts and cell behavior within the hydrogel was followed by inversion light microscopy. Figure 8a shows typical micrographs of the fibroblasts on the hydrogel surface 1, 4, and 7 days after seeding. It is evident that some cells assumed a stretched morphology after 1 day of cell culture while others still showed their original round morphology. Extensive spreading was observed after 4 days, and a marked increase in cell number was noted after 7 days of cell culture. Such results are comparable with those for several peptide-modified polymers, which alone are nonadhesive to cells.[6,8] Quantification of cell number by WST-1 assay revealed the number of viable cells doubled from 47 200 ± 9900 after 1 day to 94 900 ± 16 900 after 7 days of cell culture (see Figure 8b). Extensive spreading of cells on the gel surface was also confirmed by environmental scanning electron microscopy (ESEM) (Figure 9a), where cell morphologies were examined in the fully hydrated state.[31] Results suggest that lysozyme gels prepared are biocompatible as they favor cell spreading and promote cell proliferation. Actin filaments are the dominant mechanical support within the cell and determine the cell morphology. F-actin staining (Figure 9b) shows stretched actin filaments (green), which align roughly in parallel with each other, indicating the development of organized actin filaments in the form of stress fibers in cells.[32] These preliminary results clearly show that our lysozyme gels are biocompatible and that they provide a viable support for the cells.

Conclusions

A protein hydrogel has formed from lysozyme under reductive conditions and its physical properties have been examined. The protein denatures and self-assembles to form β-sheet-rich fibrils that become entangled to form a three-dimensional hydrogel with an average pore size of 25.6 nm and mechanical properties comparable to natural biopolymers. The formation of the β-sheet-rich fibrils is an irreversible process; however, their aggregation and formation of physical cross-links that produce the gel is thermally reversible. It has to be noted that the gels obtained meet the criteria proposed by Daniel et al.[33] for the definition of thermoreversible gels.[27] Cell culture work has shown the resulting matrix was biocompatible, promoting cell attachment, spreading, and proliferation. In comparison with polymer cell scaffolds, the preparation procedure of this protein hydrogel is simple as there is no need for the additional incorporation of cell-adhesive peptide sequences, while the cell-

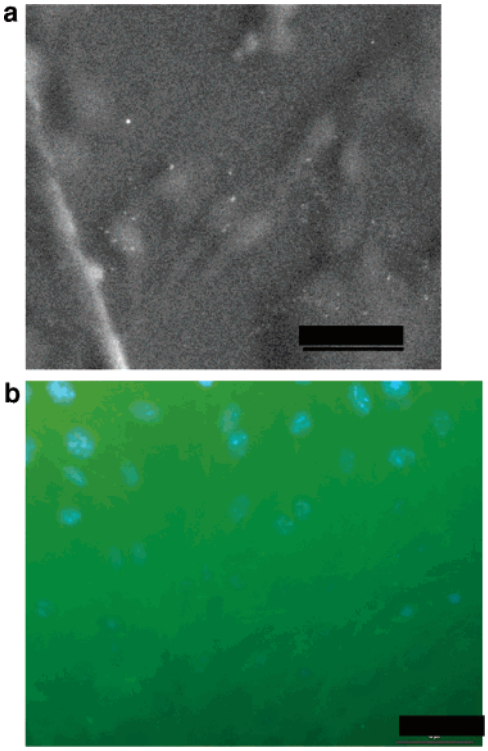

Figure 9. (a) ESEM micrograph of fibroblast cells on the surface of a 3 mM lysozyme gel at 5 °C and 6 Torr. (b) F-actin staining by FITC phalloidin under the fluorescence microscope where stretched actin filaments (green) are visible. Scale bars in both micrographs represent 50 μm.

adhesive properties are comparable. This paper indicates an alternative strategy of using proteins as building blocks to construct novel materials and represents a new class of cell scaffold that could play an important role in the biomaterial and tissue engineering sector.

Acknowledgment. We gratefully acknowledge financial support from the EU 6th Framework Marie Curie Early Stage Training Program (ExPERT). We also thank Dr. Patrick Hill (School of Chemical Engineering and Analytical Science, The University of Manchester, U.K.) for assistance with cryo-SEM work, Mr. Francis Carabine (School of Materials, The University of Manchester, U.K.) for assistance with cell culture, and Dr. Henrich Frielinghaus (Forshungszentrum Jülich, Germany) for his help with the SANS experiments.

References and Notes

(1) Halstenberg, S.; Panitch, A.; Rizzi, S.; Hall, H.; Hubbell, J. A. *Biomacromolecules* **2002**, *3*, 710−723.
(2) Hirano, Y.; Mooney, D. J. *Adv. Mater.* **2004**, *16*, 17−25.
(3) Peppas, N. A. *Advances in Chemical Engineering*; Elsevier: New York, 2004; Vol. 29.
(4) Hersel, U.; Dahmen, C.; Kessler, H. *Biomaterials* **2003**, *24*, 4385−4415.
(5) Kong, H.; Mooney, D. J. *Polysaccharides* **2005**, 817−837.
(6) Zhu, J. M.; Beamsih, J. A.; Tang, C.; Kottke-Marchant, K.; Marchant, R. E. *Macromolecules* **2006**, *39*, 1305−1307.
(7) ten Cate, M. G. J.; Rettig, H.; Bernhart, K.; Borner, H. G. *Macromolecules* **2005**, *38* (26), p 10643−10649.
(8) Dankers, P. Y. W.; Harmsen, M. C.; Brouwer, L. A.; Van Luyn, M. J. A.; Meijer, E. W. *Nat. Mater.* **2005**, *4*, 568−574.
(9) Santiago, L. Y.; Nowak, R. W.; Rubin, J. P.; Marra, K. G. *Biomaterials* **2006**, *27*, 2962−2969.
(10) Han, D. K.; Hubbell, J. A. *Macromolecules* **1997**, *30*, 6077−6083.
(11) Hern, D. L.; Hubbell, J. A. *J. Biomed. Mater. Res.* **1998**, *39*, 266−276.
(12) Jayawama, V.; Ali, M,; Jowitt, T. A.; Miller, A. F.; Saiani, A.; Gough, J. E.; Ulijn. R. V. *Adv. Mater.* **2005**, *18*, 611−614.
(13) Aggeli, A.; Bell, M.; Boden, N.; Keen, J. N.; Knowles, P. F.; McLeish, T. C. B.; Pitkeathly, M.; Radford, S. E. *Nature* **1997**, *386*, 259−262.
(14) Ozbas, B.; Rajagopal, K.; Schneider, J. P.; Pochan, D. J. *Phys. Rev. Lett.* **2004**, *93*.
(15) Haines, L. A.; Rajagopal, K.; Ozbas, B.; Salick, D. A.; Pochan, D. J.; Schneider, J. P. *J. Am. Chem. Soc.* **2005**, *127*, 17025−17029.
(16) Kasai, S.; Ohga, Y.; Mochizuki, M.; Nishi, N.; Kadoya, Y.; Nomizu, M. *Biopolymers* **2004**, *76*, 27−33.
(17) Gosal, W. S.; Clark, A. H.; Pudney, P. D. A.; Ross-Murphy, S. B. *Langmuir* **2002**, *18*, 7174−7181.
(18) Gosal, W. S.; Clark, A. H.; Ross-Murphy, S. B. *Biomacromolecules* **2004**, *5*, 2408−2419.
(19) Gosal, W. S.; Clark, A. H.; Ross-Murphy, S. B. *Biomacromolecules* **2004**, *5*, 2420−2438.
(20) Miller, A. F. *Macromol. Symp.* **2005**, *220*, 109−114.
(21) Clark, A. H.; Ross-Murphy, S. B. *Adv. Polym. Sci.* **1987**, *83*, 57−192.
(22) Claudy, P.; Letoffe, J. M.; Bayol, A.; Bonnet, M. C.; Maurizot, J. C. *Thermochim. Acta* **1992**, *207*, 227−237.
(23) Eyles, S. J.; Radford, S. E.; Robinsons, C. V.; Dodson, C. M. *Biochemistry* **1994**, *33*, 13038−13048.
(24) Goda, S.; Takano, K.; Yamagata, Y.; Nagata, R.; Akutsu, H.; Maki, S.; Namba, K.; Yutani, K. *Protein Sci.* **2000**, *9*, 369−375.
(25) Cao, A.; Hu, D.; Lai. *Protein Sci.* **2004**, *13*, 319−324.
(26) Booth, D. R.; Sunde, M.; Bellotti, V.; Robinson, C. V.; Hutchinson, W. L.; Fraser, P. E.; Hawkins, P. N.; Dobson, C. M.; Radford, S. E.; Blake, C. C. F.; Pepys, M. B. *Nature* **1997**, *27*, 787−793.
(27) Guenet, J.-M. *Thermoreversible Gelation of Polymers and Biopolymers*; Academic Press: London, 1992.
(28) Euston, S. R. *Curr. Opin. Colloid Interface Sci.* **2004**, *9*, 321−327.
(29) Barth, A.; Zscherp, C. *Q. Rev. Biophys.* **2002**, *35*, 369−430.
(30) Guinier, A.; Fournet, G. *Small-Angle Scattering of X-rays*; John Wiley & Sons: New York, 1955.
(31) Callow, J. A.; Osborne, M. P.; Callow, M. E.; Baker, F.; Donald, A. M. *Colloids Surf., B: Biointerfaces* **2003**, *27*, 315−321.
(32) Faulstich, H.; Zobeley, S.; Bentrup, U.; Jockusch, B. M. *J. Histochem. Cytochem.* **1989**, *37*, 1035−1045.
(33) Daniel, C.; Dammer, C.; Guenet, J. M. *Polymer* **1994**, *35*, 4243−4246.

BM0605560